Received: 3 May 2018 | Accepted: 7 May 2018

DOI: 10.1002/jez.2182

RESEARCH ARTICLE

WILEY JEZ-A ECOLOGICAL AND INTEGRATIVE PHYSIOLOGY

Morphological and kinematic specializations of walking frogs

Crystal M. Reynaga[1] | Henry C. Astley[2] | Emanuel Azizi[1]

[1]Department of Ecology and Evolutionary Biology, University of California, Irvine, Irvine, California

[2]Biomimicry Research & Innovation Center, Departments of Biology and Polymer Science, University of Akron, Akron, Ohio

Correspondence
Crystal M. Reynaga, Department of Ecology and Evolutionary Biology, University of California, Irvine, 321 Steinhaus Hall, Irvine, CA 92697.
Email: reynagac@uci.edu

Funding information
Department of Ecology and Evolutionary Biology, University of California, Irvine; Graduate Division, University of California, Irvine; Office of Postsecondary Education, Grant/Award Number: FG18491; Division of Integrative Organismal Systems, Grant/Award Numbers: IOS-1051691, IOS-642428; School of Biological Sciences, University of California, Irvine; Division of Graduate Education, Grant/Award Number: DGE-1321846

Grant sponsor: National Science Foundation; Grant sponsor: Department of Education; Grant sponsor: University of California, Irvine; Grant sponsor: Bushnell Research and Education Fund; Grant sponsor: Sigma Xi; Grant number: GIAR-G20111015158192.

Abstract

The anuran body plan is defined by morphological features associated with saltatory locomotion, but these specializations may have functional consequences for other modes of locomotion. Several frog species use a quadrupedal walking gait as their primary mode of locomotion, characterized by limbs that move in diagonal pairs. Here, we examine how walking species may deviate from the ancestral body plan and how the kinematics of a quadrupedal gait are modified to accommodate the anuran body plan. We use a comparative analysis of limb lengths to test the hypothesis that quadrupedal anurans shift away from the standard anuran condition defined by short forelimbs and long hindlimbs. We also use three-dimensional high-speed videography in four anuran species (*Kassina senegalensis*, *Melanophryniscus stelzneri*, *Phrynomantis bifasciatus*, and *Phyllomedusa hypochondrialis*) to characterize footfall patterns and body posture during quadrupedal locomotion, measuring the angle and timing of joint excursions in the fore- and hindlimb during walking to compare kinematics between limbs of disparate lengths. Our results show frogs specialized for walking tend to have less disparity in the lengths of their fore- and hindlimbs compared with other anurans. We find quadrupedal walking species use a vertically retracted hindlimb posture to accommodate their relatively longer hindlimbs and minimize body pitch angle during a stride. Overall, this novel quadrupedal gait can be accommodated by changes in limb posture during locomotion and changes in the relative limb lengths of walking specialists.

KEYWORDS
anura, body posture, locomotion, limb morphology, limb posture, quadrupedal

1 | INTRODUCTION

The ancestral anuran body plan is thought to reflect specializations associated with jumping, with many morphological features retained in modern frogs (Emerson, 1988; Gans & Parsons, 1966; Jenkins & Shubin, 1998; Shubin & Jenkins, 1995). Anurans tend to have short and stout bodies with relatively short forelimbs and long powerful hindlimbs, which are used to perform work against the ground during the jump take-off phase (Emerson, 1988; Peplowski & Marsh, 1997; Zug, 1972). Previous work suggests these anatomical mechanisms contribute significantly to frog jump performance (Astley, 2016; Choi, Shim, & Ricklefs, 2003; Gomes, Rezende, Grizante, & Navas, 2009; Marsh, 1994; Zug, 1978).

Despite the conservation of the ancestral body plan, anuran species have evolved several locomotor modes, each associated with novel morphological features. For example, a group of specialized burrowers have evolved tough metatarsal tubercles (spades) that aid in excavating dry soil (Emerson, 1976), a feature that appears to date back to the Paleocene (Chen, Bever, Yi, & Norell, 2016). Moreover, two arboreal families have independently evolved the ability to glide from the canopy by increasing the surface area of hands and feet with increased webbing between digits (Emerson & Koehl, 1990). The pelvic girdle morphology is one feature that does vary substantially across anurans (Emerson, 1979; Jorgensen & Reilly, 2013; Reilly & Jorgensen, 2011). Emerson (1979) described three pelvic configurations that were proposed to correlate with locomotor mode, which shows a strong correlation between the sacral diapophyses width and an animal's locomotor specialization (Jorgenson and Reilly, 2013). The evolution of novel locomotor modes rarely eliminates jumping from an anuran's locomotor repertoire, resulting in specific morphological modifications without large-scale changes in the general body plan (Emerson, 1988).

Several frog species have independently evolved walking as a primary mode of locomotion. This gait is characterized by limbs moving in alternating, diagonal pairs (Ahn, Furrow, & Biewener, 2004; Emerson, 1979). In one species, *Kassina maculata*, the kinetics and energy exchange of the quadrupedal gait resemble a walk at slow speeds and shift to a run-like gait at higher speeds (Ahn et al., 2004). Although the authors did not quantify joint level limb kinematics, they noted the limb posture appeared highly crouched across speeds (Ahn

et al., 2004). A crouched limb posture is quite common in smaller quadrupedal mammals (Biewener, 1989a). In contrast, larger mammals with more extended limbs operate with higher effective muscle mechanical advantage, allowing them to support a larger body mass during locomotion (Biewener, 1989a).

Interestingly, a comparative analysis also suggests limb posture (effective mechanical advantage) does not differ between the mammalian fore- and hindlimbs (Biewener, 2005). This observation is not particularly surprising given the fore- and hindlimbs of many quadrupedal mammals are typically of similar length (Biewener, 1983). The symmetry in limb length does decrease in smaller mammals that tend to have slightly longer hindlimbs compared with their forelimbs (Biewener, 2005). This shift away from symmetric limb lengths is not restricted to smaller quadrupedal mammals but also extends to locomotor specializations such as bipedal running, hopping, vertical clinging and leaping. One such example is the *Galago senegalensis*, which is an arboreal primate with legs almost twice the length of its forelimbs (Preuschoft, Witte, & Fischer, 1995). The asymmetry in the limb lengths of the galago is associated with its ability to perform exceptionally powerful jumps (Aerts, 1998), but this species largely avoids the use of a quadrupedal walking gait (Napier & Walker, 1967). It is therefore likely that high asymmetry in limb length fundamentally alters the limb posture, limb mechanical advantage, and body posture in species that utilize a quadrupedal gait.

The independent evolution of walking in many anuran lineages presents a unique opportunity to investigate how the ancestral body plan, associated with jumping, likely constrains limb and body postures during a quadrupedal gait. We combine a broad comparative morphological approach with detailed kinematics of four independently derived species of specialized anuran walkers to determine how the conflicts associated with an anuran body plan are accommodated by species that commonly use a quadrupedal gait (Figure 1). We propose three potential mechanisms that may be associated with quadrupedal walking. First, we predict species specialized for walking have more symmetric fore- and hindlimb lengths compared with other anuran species (Figure 2A). Second, we predict that if limb lengths remain asymmetric, frogs may adjust body posture by using a significant downward pitch during locomotion (Figure 2B). Finally, we predict the posture of longer hindlimbs will likely be significantly more crouched compared with the shorter forelimbs (Figure 2C). These predictions are not mutually exclusive and species may combine these strategies to circumvent the constraints of the anuran body plan. This work seeks to highlight morphological and kinematic strategies associated with the evolution of quadrupedal walking and reveal potential conflicts and trade-offs between disparate locomotor modes.

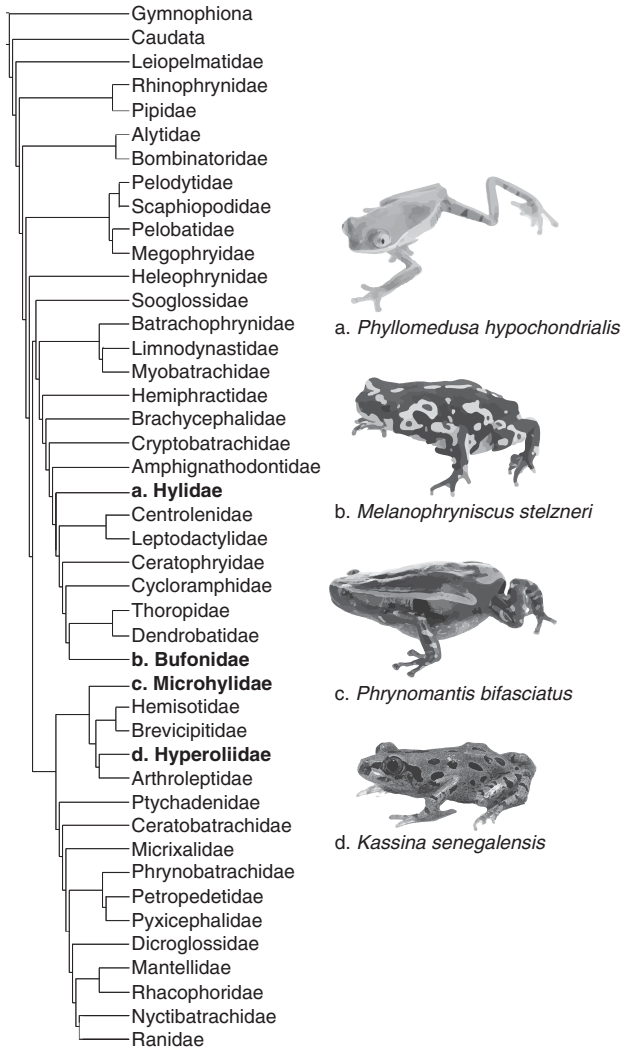

FIGURE 1 Anuran phylogenetic relationships based on Frost et al. (2006) and Isaac et al. (2012). Families of study species are in bold script. Bolded families indicate where quadrupedal walking has evolved. However, not all species within those families are specialized walkers; many still retain the ancestral jumping specialization. Lowercase letters correspond to pictured study species from independently derived lineages: (A) tiger-legged monkey frog (*Phyllomedusa hypochondrialis*), (B) bumblebee toad (*Melanophryniscus stelzneri*), (C) red-banded rubber frog (*Phrynomantis bifasciatus*), and (D) Senegal running frog (*Kassina senegalensis*)

2 | MATERIALS AND METHODS

We test our predictions on four independently derived lineages of specialized quadrupedal walking frogs to study variation in limb posture (Astley, 2016; Emerson, 1979; Figure 1 and Supp. Movie 1). We combine meta-analysis, direct limb measurements, and online database collections to examine evolutionary changes in limb length, and use three-dimensional (3D) high-speed kinematic video analysis to characterize the specialized walking gait, including detailed analysis of limb and body postures.

2.1 | Quadrupedal walking frogs

This study used four specialized walking frogs: the Senegal running frog, *Kassina senegalensis* ($n = 5$); the bumblebee toad, *Melanophryniscus stelzneri* ($n = 2$); the red-banded rubber frog, *Phrynomantis bifasciatus* ($n = 3$); and the tiger-legged monkey frog, *Phyllomedusa hypochondrialis* ($n = 2$). These species were chosen for their capability to perform diverse modes of locomotion (e.g., swimming, jumping); however, all four predominately utilize a quadrupedal walking gait for

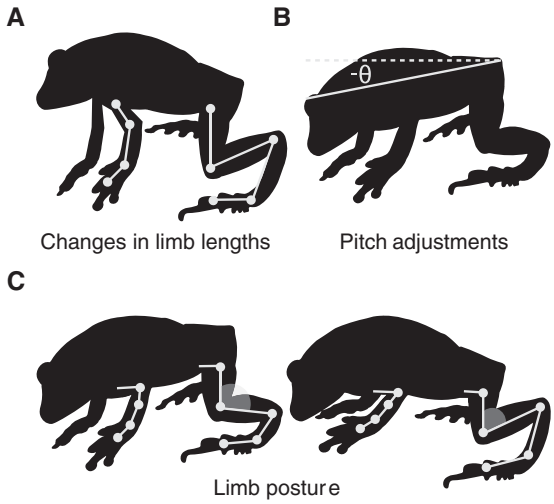

FIGURE 2 Schematic representation of three hypothetical solutions to how quadrupedal walking frogs circumvent the constraints of an anuran body plan specialized for jumping. The associated changes to achieve a quadrupedal gait can be morphologic or kinematic: (A) One way to achieve this is through more symmetric limb dimensions. Otherwise, if limb dimensions remain asymmetric frogs may adjust (B) with a downward body pitch to accommodate for a longer hindlimb. Alternatively, (C) adjust limb posture; where forelimbs assume a more flexed or extended limb posture than the hindlimbs

terrestrial, non-escape locomotion, as well as arboreal locomotion in the case of *Phy. hypochondrialis*. An extreme example is *Phr. bifasciatus*, which we rarely observed jump (personal observation). Although some other species of anurans will walk on rare occasions, this behavior is extremely infrequent and difficult to elicit consistently, particularly for repeated cycles; prior experiments by one author failed to produce walking behavior in numerous other species in the lab (Astley, 2016). Although the rarer three species had lower sample sizes, we filmed a number of trials per individual within a species to reduce intraspecific error via repeated-measures statistics (see Table 1).

Filming and animal husbandry for *K. senegalensis* were conducted at the University of California, Irvine (UCI) and approved by the UCI Institutional Animal Care and Use Committee (IACUC). Filming and animal husbandry for *M. stelzneri*, *Phr. bifasciatus*, and *Phy. hypochondrialis* were conducted at Brown University and approved by the Brown University IACUC. Videos filmed at Brown University were originally used for previous study by Astley (2016). All species were wild-caught and purchased from commercial vendors.

2.2 | Limb morphological measurements

We sampled a diverse array of anurans to assess whether species that specialize in quadrupedal walking have more symmetric fore- and hindlimb lengths compared with a range of other anuran species. Specimens came from the collections of Herpetology at the Natural History Museum of Los Angeles County (LACM), the online National Science Foundation Digital Library at the University of Texas at Austin (DigiMorph), and personal collections. We collected fore- and hindlimb measurements from 56 anuran species spread across 14 major families. For specimen information, see Supp. Table S1. Whenever possible, we examined multiple individuals per species ($n = 1–10$) to characterize the range of limb dimensions. We examined either cleared and stained specimens, dry skeletal preparations, or 3D X-ray computed tomography (CT) scans.

We calculated limb lengths from the sum of the lengths of each individual limb element. All measurements were straight line measurements of the skeletal elements; the distance from the most proximal end to the most distal end. We measured three forelimb segments: the humerus, radio-ulna, and metacarpophalangeal segment; and in the hindlimb: the femur, tibiofibula, proximal tarsal, and metatarsophalangeal segment. We measured the most distal segment length as the linear distance from the proximal end of the metacarpus (or metatarsus) to the distal end of the longest phalanx. We measured all prepared specimens with digital calipers, and recorded to the nearest 0.01 mm. For measurements on 3D X-ray CT specimens, we used Java slice applet viewer application, the UTCT inspeCTor (Digital Morphology, Austin, TX). We used *X*, *Y*, *Z* coordinates to calculate limb segment lengths.

TABLE 1 Average walking anuran performance values (Mean ± SEM)

Species	Individual	Trials	SNVL (mm)	Mass (g)	L_{stride} (cm)	V_{stride} (cm/sec)
K. senegalensis	1	5	28.02	1.64	4.42 ± 0.28	21.29 ± 1.95
	2	5	35.41	2.34	3.85 ± 0.26	12.20 ± 2.05
	3	5	29.69	1.87	4.11 ± 0.20	20.66 ± 1.83
	4	5	33.32	2.38	4.32 ± 0.57	19.14 ± 3.34
	5	5	30.94	1.53	3.74 ± 0.38	14.43 ± 2.71
M. stelzneri	1	2	29.47	1.58	2.95 ± 0.22	16.84 ± 1.90
	2	4	22.00	0.82	3.00 ± 0.33	15.65 ± 1.23
Phr. bifasciatus	1	5	41.15	4.17	4.34 ± 0.51	15.65 ± 1.23
	2	5	39.37	3.92	5.13 ± 0.16	23.65 ± 3.58
	3	5	41.99	4.78	3.15 ± 0.13	5.13 ± 0.27
Phy. hypochondrialis	1	5	37.25	2.28	5.43 ± 0.42	11.68 ± 1.50
	2	5	34.25	1.99	4.69 ± 0.13	16.18 ± 2.77

SNVL, snout-vent length; L_{stride}, stride length; V_{stride}, stride velocity. See Supp. Table S1 for average limb length details.

Furthermore, we used meta-data from Mammalia to assess whether specialized walking anuran species have similar limb length symmetry to mammalian quadrupeds. Data came from a previously published study by Biewener (1983). These data from 33 mammalian quadrupedal locomotors approximate mammalian limb lengths from measurements of the radius, humerus, tibia, and femur lengths. For mammals, the bones contained in the terminal end of the fore- and hindlimb, such as tarsals, metatarsals, and phalanges, were not included in total limb length calculations. However, the bony elements that make up the associated metatarsal joint below the foot or ankle contribute negligibly to the total limb length or center of mass in mammals (Steudel & Beattie, 1993).

2.3 | Walking kinematics and analysis

We collected all 3D video kinematic data under standardized conditions at approximately 23 ± 2°C at UCI and 28 ± 2°C at Brown University. In spite of temperature differences, there was some overlap in walking speed between the *K. senegalensis* trials in this study and those in Astley, 2016. We recorded the 3D kinematics of quadrupedal walking events for each species with two high-speed video cameras. We filmed events at UCI with Phantom M120 Cameras (Vision Research Inc., Wayne, NJ), whereas events filmed at Brown University used Photron 1024 PCI Cameras (Photon Inc., Tokyo, Japan). The cameras, positioned laterally and dorsally to the individual, recorded at 500 frames sec^{-1} at UCI and 125 frames sec^{-1} at Brown University, and were calibrated with a custom calibration cube (32 non-planar points) with direct-linear transformation software (Hedrick, 2008) in MATLAB (The MathWorks, Natick, MA).

We recorded walking events as the animal moved freely throughout the arena (30 × 15 cm^2). For each frog, two-dimensional (2D) data were collected from both cameras to characterize body and limb postures within a stride. To do this, we manually tracked the following joint center landmarks along one side of the body, in each frame for both recordings: the wrist, elbow, and shoulder joints in the forelimb; the ankle, knee, and hip joints in the hindlimb; the distal end of the longest phalange for each limb; the sacroiliac joint; and the centers of both eyes. 2D camera data were reconstructed to 3D with MATLAB digitizing scripts (Hedrick, 2008). We defined the arena surface as the *x*–*y* plane, with the *z*-axis perpendicular to the plane. We performed further kinematic analysis of the 3D coordinates from these anatomical landmarks using MATLAB, IGOR Pro (Wavemetrics, Inc., Beaverton, OR) and Excel (Microsoft Corp., Renton, WA). We quantitatively analyzed multiple walking stride trials per individual for each species (Table 1). Analyzed trials were carefully selected to ensure all anatomical landmarks were visible to both cameras and frogs completed at least one stride cycle without any impediments. However, frogs rarely walked exactly parallel to the *x*-axis of the arena, often times walking at a slight diagonal to the axis. Although no drastic turning events were analyzed, slight diagonal walking events introduced a small change of heading within a stride.

We used average footfall patterns within a single stride to ensure similar gait ranges were examined. We defined a single stride cycle as the video frame when the forelimb facing the laterally positioned camera touched-down, lead forelimb (LFL), to the frame just before the same LFL touched down again to begin a new stride. To characterize footfall patterns, we quantified the number of frames where touch-down and lift-off occurred for each foot, and normalized to the total frames within a stride. We used Hildebrand (1985) terminology to characterize gaits. We calculated duty factor as the average percent of a stride a single foot contacted the ground. We characterized same-side limb phase as the average percent of a stride when the hindfoot made contact with the ground until the same-side forelimb made contact with the ground.

We used absolute pitch and yaw angles to characterize body posture, with respect to the horizontal ground as a fixed plane of reference. First, we performed global to local coordinate system transformations with a custom-designed script in MATLAB. To define the 3D position of landmarks in the global reference frame, we used coordinates based on the mean position of where three phalanges encountered the platform within the filming arena. We used these landmarks to find the frog position relative to the arena platform, which were fixed with respect to the moving frog body. Second, we defined the body axis as a parasagittal line connecting the eye and the dorsal lateral projection of the sacrum, both located on the same lateral side of the body axis closest to the laterally positioned camera. Third, *Y* coordinates of the sacroiliac joint were subtracted from each eye center coordinate, so the sacroiliac joint acted as the origin of the horizontal plane. As a point of comparison with empirical data, we predicted body pitch angle based on fully extended limbs. For pitch angles, positive values indicated a body posture where the rostrum is elevated relative to the sacrum, whereas negative values indicated the sacrum is elevated relative to the rostrum. Pitch angles of zero indicated a perfectly level body posture relative to the horizontal axis. Lastly, we defined yaw angle as the angle of rotation of the body axis around the horizontal *x*-axis. For example, if a frog walked in a straight-line trajectory along the positive *x*-axis direction, a yaw angle of zero assumes the body axis is perfectly aligned with the *x*-axis. However, positive changes in yaw indicated the rostrum was angled toward the left side of the sacroiliac joint, whereas negative values indicated the rostrum was directed toward the right side of the sacroiliac joint. Additionally, we accounted for slight changes in heading within a stride by characterizing the net change in frog head orientation at the start and end of a stride.

We calculated relative 3D joint angles between segments listed below, which were not separated into flexion/extension and adduction/abduction components nor referenced to body position. We measured wrist angle as the angle between the metacarpals and radio-ulna; elbow angle, the angle between the radio-ulna and humerus; shoulder angle, the angle between the humerus and the ipsilateral eye; ankle angle, the angle between the tarsus and tibiofibula; knee angle, the angle between the tibiofibula and femur; and the hip angle, the angle between the femur and the ipsilateral sacroiliac joint. For joint angles, values closer to 0° indicated greater joint flexion and values closer to 180° indicated greater extension.

We also characterized 3D limb postures within the local reference frame of the fore- and hindlimb (Figure 3). First, coordinates of the distal phalange were subtracted from either the shoulder or hip

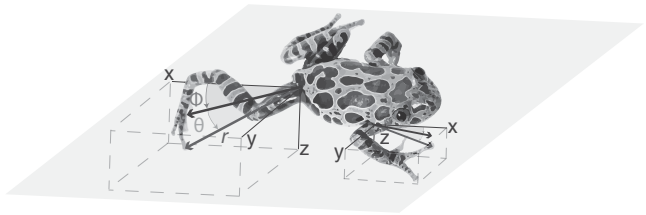

FIGURE 3 Schematic diagram of the coordinate system used to characterize 3D limb posture. Polar coordinates were used to characterize the radial distance, *r*, the magnitude of limb extension from the shoulder and hip. Then, the vertical protraction of the limb was characterized by the elevation angle, θ. Lastly, the lateral abduction of the limb was characterized by the azimuth angle, ϕ

joints respectively to make the joints the origins of the coordinate axes for each limb. Then, 3D Cartesian coordinates of the digitized body landmarks were transformed to spherical coordinates. Angular changes in this coordinate system were defined as the radial magnitude (*r*), elevation, and azimuth. We calculated the aforementioned fore- and hindlimb polar angles from a 3D vector directed from the shoulder or hip to the tip of the longest phalanx. The azimuth angle characterized the lateral abduction or adduction of the limbs where larger angle indicated laterally abducted limb posture. The elevation angle characterized the vertical protraction or retraction of the limb, where a larger angle corresponded with a vertically protracted limb posture. The variable *r* was defined as the instantaneous distance from the most proximal joint to the most distal digit tip. Elevation, azimuth, and *r* were calculated for all frames for both fore- and hindlimb. Lastly, we normalized *r* by dividing the total limb length (*r*: total limb length). By normalizing *r*, this measured how flexed or extended the limb was on a scale from 0 to 1, respectively. We evaluated these variables at mid-stance and at maximum *r*, during the period of ground contact for each limb. The timing of maximum *r* within a stride for the forelimb coincided with touch down, whereas for the hindlimb maximum *r* occurred during the take-off phase of the hindlimb within a stride, and thus do not occur at the same instant in time. Relative 3D joint angle measurements were also taken at midstance and maximum *r* relative to each limb. Ranges between midstance and maximum *r* and means during stance phase were also calculated for relative 3D joint angles.

2.4 | Statistical analysis

We analyzed all data with RStudio (v. 1.0.136, Boston, MA) and IGOR Pro. We calculated all species means and standard errors from individual means. For the comparative analysis, we grouped species into locomotor type: quadrupedal walking anurans, other anuran locomotors, and quadrupedal mammals. Fore- and hindlimb lengths were $\log_{10}$ transformed prior to analysis. We calculated least-squares regressions to determine the relationship between mammalian quadruped fore- and hindlimb lengths. We used phylogenetic generalized least squares (PGLS) to control for similar traits and shared evolutionary history across anuran locomotor groups (Garland & Ives, 2000; Grafen, 1989; Martins & Hansen, 1997). We used packages CAPER, APE, and NLME in R for PGLS and to assess phylogenetic contribution (Orme et al., 2013; Paradis, Claude & Strimmer, 2004; Pinheiro, Bates, DebRoy, & Sarkar, 2017). PGLS used a pruned phylogeny (modified in R) from published phylogenetic analyses (Frost et al., 2006; Isaac, Redding, Meredith, & Safi, 2012). Traits were assumed to evolve by "Brownian motion" evolution (Rohlf, 2001). Furthermore, we used analysis of covariance (ANCOVA) to test for differences between anuran locomotor groups, with forelimb length as the covariate and locomotor type (walker versus other specialized anuran locomotor) as the fixed factor. ANCOVA was performed on log transformed data not corrected for phylogeny to determine what model best fit the data to test our hypothesis. Fit of PGLS and ANCOVA models were compared with Aikake information criterion (AIC).

For the kinematic data set, we calculated averages and 95% confidence intervals for pitch, yaw, relative joint angles, limb extension magnitude (*r*), and polar limb angles from individual means. We used one-way analysis of variance (ANOVA) to compare pitch and joint angles across species, accounting for variance across individuals. To test for differences in 3D limb postures, *r*, azimuth, and elevation angles, we used repeated measures ANOVA, accounting for variance within individuals, with a false discovery rate *post hoc* test.

3 | RESULTS

3.1 | Limb morphology

We sampled a diverse array of anuran species to characterize the relationship between fore- and hindlimb lengths of four specialized walking anuran species and 55 other anurans (Figure 4). For comparison, we included data from 33 mammalian quadruped species (Biewener, 1983). Least-squares regression indicated mammalian quadrupeds exhibit nearly equal fore- and hindlimb lengths with a slope closest to one (slope ± SEM = 0.926 ± 0.0117). We found a strong correlation between the mammalian fore- and hindlimb lengths ($R^2 = 0.995$; $P < 0.0001$). In multivariate analyses, anuran hindlimb length scaled nearly isometrically with forelimb length (slope ± SEM = 0.941 ± 0.047; see Supp. Table S2). The regression lines show a significant effect of forelimb length and locomotor type, but no significant interaction. These results suggest that the slope between fore- and hindlimb length is similar for all anurans regardless of locomotor type (see Supp. Table S2; ANCOVA: $P = 0.738$; PGLS: $P = 0.846$). However, locomotor type has a significant effect on hindlimb length, with a significant difference in the regression line intercepts (see Supp. Table S2; ANCOVA: $P = 0.0003$; PGLS: $P = 0.005$). PGLS was the best-fitting regression model based on the smallest AIC value (see Supp. Table S2). For Anura, Pagel's lambda indicated limb proportions were correlated with phylogeny (see Supp. Table S2). This confirmed anuran quadrupedal walkers have more equal limb lengths compared with other anurans.

3.2 | Footfall patterns

We examined footfall patterns to verify whether each species (*K. senegalensis*, *M. stelzneri*, *Phy. hypochondrialis*, and *Phr. bifasciatus*) used a similar walking or running gait (Figure 5). All four quadrupedal walking

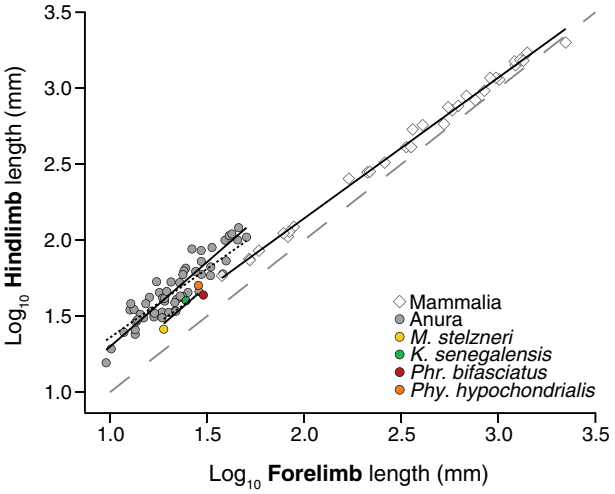

FIGURE 4 The relationship between log-transformed fore- and hindlimb length of quadrupedal walking frogs ($N = 4$), relative to other specialized anuran locomotors ($N = 56$) and mammalian quadrupeds ($N = 33$). Each symbol represents a different species. See Supp. Table S1 for details on plotted anuran species. The gray dashed line is the line of isometry, with a slope of one, it indicates equal lengths between fore- and hindlimb. Approximate limb lengths (radius, humerus, tibia, and femur) of Mammalia are displayed for reference, obtained from Biewener (1983). We calculated solid regression lines from log-transformed data points shown, whereas dotted regression lines are based on PGLS. These results demonstrate quadrupedal walking anurans appear to have more equal fore- and hindlimb lengths. PGLS statistics are given in Supp. Table S2 [Color figure can be viewed at wileyonlinelibrary.com]

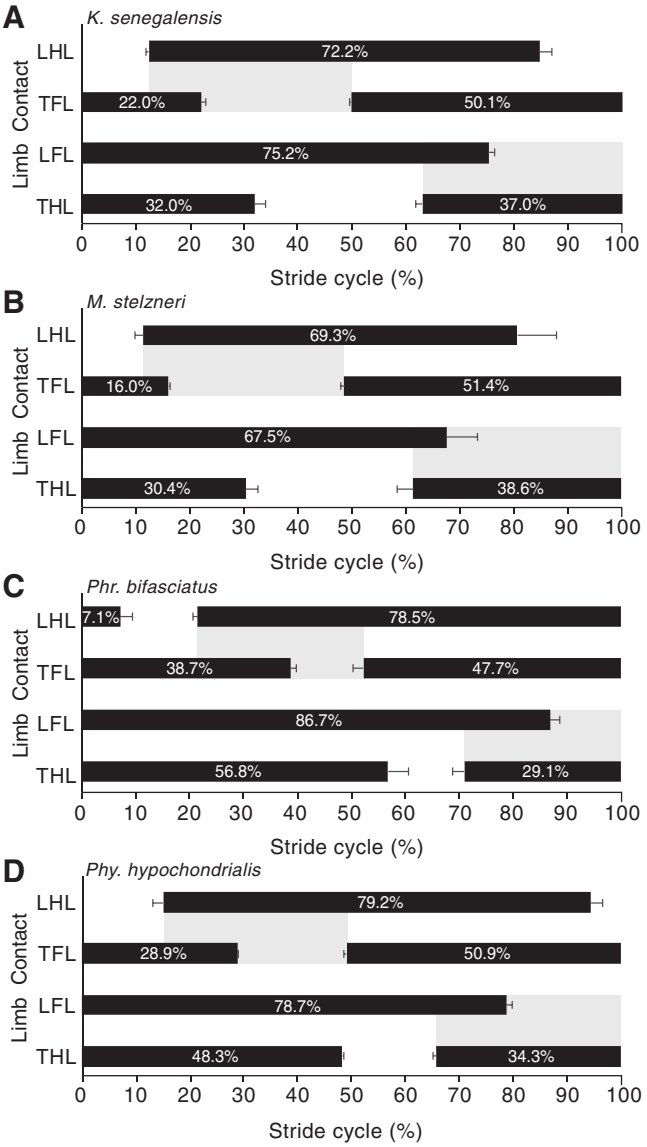

FIGURE 5 Average footfall patterns over a single stride (mean ± SEM). Mean and standard error calculated from video frames normalized to stride duration. (A) *Kassina senegalensis* ($n = 5$), (B) *Melanophryniscus stelzneri* ($n = 2$), (C) *Phrynomantis bifasciatus* ($n = 3$), and (D) *Phyllomedusa hypochondrialis* ($n = 2$). Stride cycle was defined from the first point of contact from the leading forelimb (LFL), to just before the same LFL touched back down for a new stride. The footfall order is the LFL, leading hindlimb (LHL), trailing forelimb (TFL), and trailing hindlimb (THL). Dashed lines indicate same-side limb phase used to characterize locomotor gait in Figure 6. The footfall patterns show these walking frog species use similar alternating limb movements

species used a diagonal footfall sequence, where the movement for a given forelimb was followed by the contralateral hindlimb. The gait cycles analyzed between forelimb and contralateral hindlimb pairs alternated in sequence. At any given time within a stride, the frogs had two limbs or more in contact with the ground. According to footfall sequence, duty factor varied across species with the fastest duty factor by *M. stelzneri* and *K. senegalensis*, which overlapped in their range, whereas *Phr. bifasciatus* had the lowest duty factor (Figure 6). Although Ahn et al., 2004 observed grounded running in *K. maculata* at duty factors above 50%, we refer to these sequences as "walking" for consistency, based on our measured duty factor. *Phr. bifasciatus* predominately used a single foot sequence walk, whereas *K. senegalensis*, *M. stelzneri*, and *Phy. hypochondrialis* mainly used a diagonal couplet footfall sequence.

3.3 | Body posture

We measured body pitch across quadrupedal walking species to determine whether these frogs modulate pitch angle to accommodate for the difference between the fore- and hindlimb lengths. Comparisons were made relative to predicted body pitch angles for each species. Predicted body pitch angles were calculated from total anatomical fore- and hindlimb lengths (assuming full limb extension) and illustrated as a point of comparison with the observed body pitch across a stride (Figure 7). All quadrupedal walkers showed little variation in pitch. Pitch angles did not deviate from zero enough to reach predicted negative pitch values. Despite limb asymmetry, the boxes combined with whiskers indicated nonsignificant difference in body pitch across species (one-way ANOVA; $P = 0.995$). Although pitch angles did not deviate significantly from a horizontal orientation, we did detect consistent yaw (average range: *K. senegalensis* −15.0 ± 2.5° to 7.4 ± 0.8°; *M. stelzneri* −11.0 ± 3.5° to 4.0 ± 0.2°; *Phr. bifasciatus* −5.7 ± 1.1° to 7.1 ± 2.6°; *Phy. hypochondrialis* −5.4 ± 9.8° to 14.5 ± 4.8°) throughout the stride cycle (Figure S1A–D). Yaw angles frequently returned to a

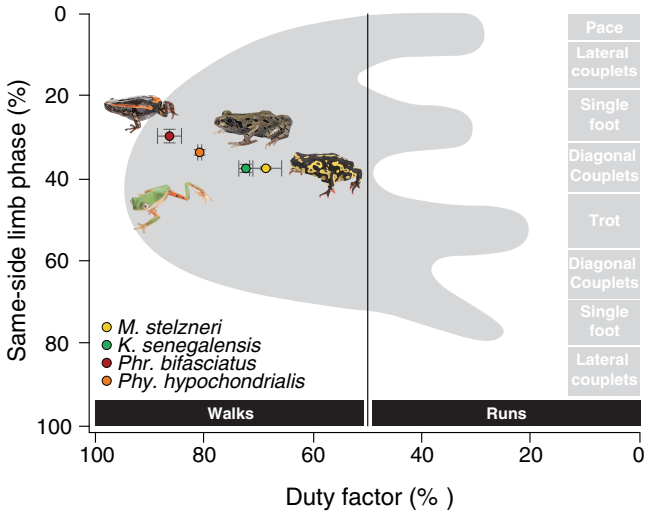

FIGURE 6 Average walking gaits of four quadrupedal walking frog species (Mean ± SEM): *Kassina senegalensis* (green; $n = 5$), *Melanophryniscus stelzneri* (yellow; $n = 2$), *Phrynomantis bifasciatus* (maroon; $n = 3$), and *Phyllomedusa hypochondrialis* (orange; $n = 2$). Footfall patterns were solely used to characterize walking patterns. All species used a walking gait with either single foot or diagonal couplet sequence limb phases. Plot adapted from Hildebrand (1980) [Color figure can be viewed at wileyonlinelibrary.com]

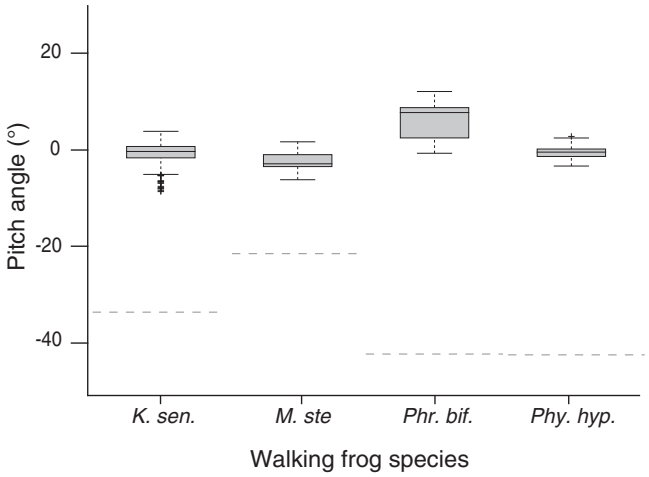

FIGURE 7 Comparison of average body pitch within a stride cycle and estimated body pitch from total extended limb lengths. (A) *Kassina senegalensis* (green; $n = 5$), (B) *Melanophryniscus stelzneri* (yellow; $n = 2$), (C) *Phrynomantis bifasciatus* (maroon; $n = 3$), and (D) *Phyllomedusa hypochondrialis* (orange; $n = 2$). Box plots correspond to changes in body pitch over a stride duration. Box-and-whisker diagrams show body pitch variation within a single stride. The boxes represent 50% of the data range, whiskers represent the interquartile range, bold horizontal bars represent the median, box height and whisker asymmetry indicate skewness of observations. The dashed line is the predicted pitch angle, calculated from total limb length. For all four species, pitch angle hardly deviated from 0 and differed from estimated pitch angles

value of zero at the beginning of a new stride. However, when frogs were not walking in a perfectly straight line, yaw angles did not return to zero at the stride transition (Figure S1E–H).

3.4 | Limb posture

We measured joint kinematics to examine how forelimb extension or hindlimb flexion may compensate for unequal fore- and hindlimb lengths (Figure 8; Supp. Figure S2 and Table S3). From joint coordinates across each limb, we measured relative joint angle extension and flexion across a stride. All frogs used similar fore- and hindlimb joint angle patterns (see Supp. Table S3). Specifically, forelimb joint angle changes followed a similar pattern in the proximo-distal direction with average joint angles only varying across species at the wrist ($P = 0.0103$). At mid-stance, elbow angle across species significantly differed ($P = 0.0492$), largely driven by greater elbow joint extension in *M. stelzneri* (Supp. Table S3). Likewise, hindlimb joint angles follow similar magnitudes. However, *Phr. bifasciatus* and *Phy. hypochondrialis* deviate in the timing of hindlimb joint excursion. This shift in hindlimb timing is also reflected their footfall patterns illustrated in Figure 5. Average ankle angle significantly differed across species ($P = 0.0024$), largely due to a reduced joint angle in *Phy. hypochondrialis* (Supp. Table S3). A difference in hip joint range across species resulted from a smaller relative hip joint angle range in *Phr. bifasciatus* (Supp. Table S3).

We also examined the fore- and hindlimb postures by characterizing the magnitude of limb extension, lateral abduction, and vertical retraction by using spherical coordinates and reducing the limb to a 3D vector characterized by the magnitude of the vector (r), the elevation angle, and the azimuth angle across a stride (Figure 3 and Supp. Figure S3). We measured these variables at mid-stance and at maximum limb extension (Figure 9). The ratio of the vector magnitude to the total limb length (r:TL) was used to estimate the amount of limb flexion. At mid-stance, elevation angle across all species were greater in the forelimb relative to the hindlimb (Figure 9A; $F = 292.67$, $P < 0.0001$). Post-hoc tests showed differences across species were largely driven by variation in hindlimb retraction (Supp. Table S4). Moreover, a significant interaction between species and limb suggested the elevation angle difference between the fore- and hindlimbs were different across species ($F = 32.28$, $P = 0.0014$). Between species azimuth angle in the fore- and hindlimb at mid-stance were different (Figure 9B; $F = 11.96$, $P = 0.0124$). Consequently, post hoc tests revealed that differences across species were largely driven by greater lateral forelimb abduction in *K. senegalensis* (Supp. Table S4, $P = 0.002$). Lastly, r:TL differed between species (Figure 9C; $F = 11.18$, $P = 0.014$), however there was no difference between relative extension of fore- and hindlimbs within species. A significant interaction suggested that the relative extension of the fore- and hindlimb for each species were different ($F = 9.369$, $P = 0.020$), likely attributed to the slight variation in forelimb flexion and hindlimb extension in *M. stelzneri* and *Phr. bifasciatus* (Supp. Table S4).

At maximum limb r, elevation angle of the fore- and hindlimb differed between species (Figure 9D; $F = 6.124$, $P = 0.045$), and within species ($F = 60.46$, $P = 0.0006$). There was a significant interaction between species and limb ($F = 33.70$, $P = 0.0013$). This result was largely driven by a significant decrease in forelimb elevation angle relative to the hindlimb in *Phr. bifasciatus* ($P = 0.005$) and *Phy. hypochondrialis* ($P = 0.028$) whereas, in *K. senegalensis* and *M. stelzneri*, both the fore- and hindlimbs achieved similar elevation

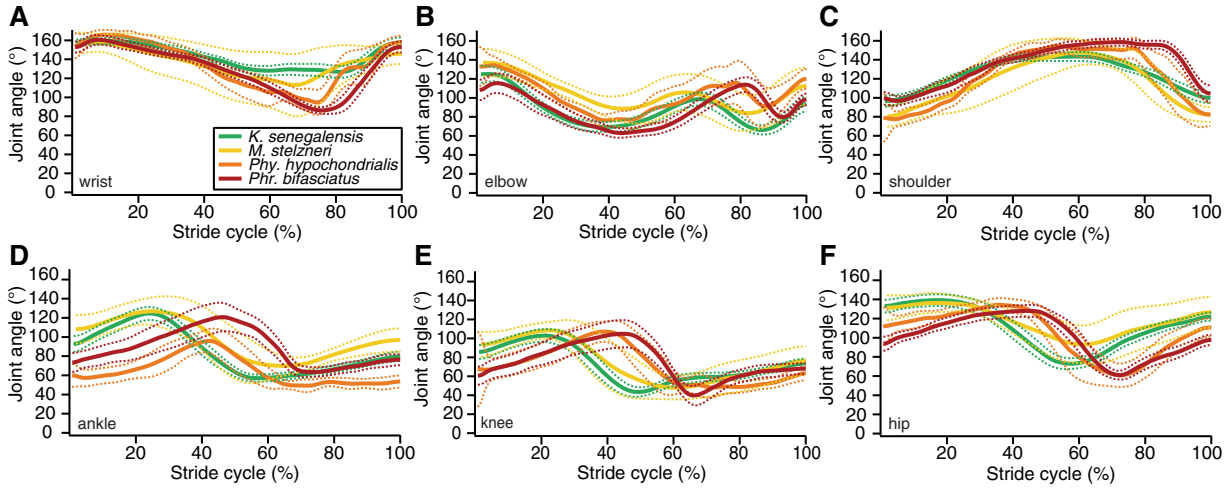

FIGURE 8 Average relative joint angle changes over a stride in the fore- and hindlimb. *Kassina senegalensis* (green; $n = 5$), *Melanophryniscus stelzneri* (yellow; $n = 2$), *Phrynomantis bifasciatus* (maroon; $n = 3$), and *Phyllomedusa hypochondrialis* (orange; $n = 2$). The top row of graphs shows the joint angle changes in the forelimb: (A) wrist, (B) elbow, and (C) shoulder. The bottom row of graphs shows joint angle changes in the hindlimb: (D) ankle, (E) knee, and (F) hip. A complete stride cycle is defined from the first point of contact of the leading forelimb to just before the same leading forelimb touches back down. All averaged data are shown as a solid line, with dotted lines that represent 95% confidence intervals. Relative joint angle patterns are similar across species, however deviates in the timing of these changes throughout a stride. See Supp. Figure S2 for reproduced figure with individual joint angle trail traces [Color figure can be viewed at wileyonlinelibrary.com]

angles. Though there was no difference between species in azimuth angle, within species fore- and hindlimb azimuth angles differed (Figure 9E; $F = 12.82$, $P = 0.016$). There is a significant interaction of species and limb, suggesting this difference between fore- and hindlimb azimuth angle are different across species. At maximum extension, fore- and hindlimb abduction were similar for *K. senegalensis*, whereas fore- and hindlimb azimuth angles began to further differentiate in *M. stelzneri* ($P = 0.0006$), *Phr. bifasciatus* ($P = 0.0009$), and *Phy. hypochondrialis* ($P = 0.0024$). At maximum *r*, *r*:TL, effective use of limbs differed between species (Figure 9F; $F = 9.738$, $P = 0.0189$), with a significant difference in effective use of fore- and hindlimbs ($F = 16.93$, $P = 0.009$). The interaction of species and limb suggests species are changing fore- to hindlimb flexion and extension relative to one another in different ways at maximum extension ($F = 26.91$, $P = 0.002$), however each species effectively uses the entire length of the fore- and hindlimb similarly.

4 | DISCUSSION

Our results support the hypothesis that quadrupedal walking frogs have more equal fore- and hindlimb lengths compared with other anurans (Figure 4). It is clear that phylogeny and locomotor type are critical predictors of hindlimb lengths in anurans. PGLS regression provides a better fit of the data compared with a standard ANCOVA, and indicate frogs specialized in quadrupedal walking have significantly reduced asymmetry in fore- and hindlimb lengths compared with other anurans (Supp. Table S2). This pattern is consistent with findings that suggest walking species tend to have shorter hindlimbs relative to snout vent length (Astley, 2016). Our analysis indicates fore- to hindlimb length ratios in our walking frogs are similar to those measured in small cursorial mammals (Figure 4; Biewener, 1983). Despite a shift toward symmetric limb dimensions, walkers still retain significantly longer hindlimbs compared with forelimbs. In fact, on several occasions we observed a complete walking stride impeded in *K. senegalensis* when the hindlimb actually stepped on the ipsilateral forelimb, thereby delaying the start of the next stance phase cycle (personal observation). These stride impediments were only observed in *K. senegalensis*. It is likely such interference between the fore- and hindlimbs would be more prevalent without the observed deviation from the ancestral body plan in walking species.

The footfall patterns of all four species can be characterized as a walking gait with alternating limb movements (Figure 5). Per Hildebrand's (1985) terminology these species range variably in footfall sequence within a stride (Figure 6). This is consistent with the red-legged running frog (*K. maculata*) and tiger salamander (*Ambystoma tigrinum*), which have similar kinematics to *M. stelzneri* and *K. senegalensis* (Ahn et al., 2004; Reilly, McElroy, Odum, & Hornyak, 2006). This footfall pattern is similar to patterns typically seen in short-legged mammals, which use a single-foot or diagonal-couplet gaits (Hildebrand, 1968). However, Ahn et al., 2004 showed that duty factor and footfall patterns can be inconsistent with energy exchange patterns associated with walking and running, making it somewhat difficult to formally characterize quadrupedal frog gaits. Additionally, our kinematic results indicated that footfall patterns alone do not reflect some of the nuanced features of the gait, limb and body postures arising from the significant fore–hind asymmetry in limb lengths.

We hypothesized to accommodate longer hindlimbs walking frogs may locomote with significantly more crouched hindlimbs than forelimbs. We find little support for this hypothesis using only observed relative joint angle kinematic comparisons in the fore- and hindlimbs (Figure 8 and Supp. Table S3). However, assessing relative joint angles to characterize limb posture is not entirely appropriate for anurans that

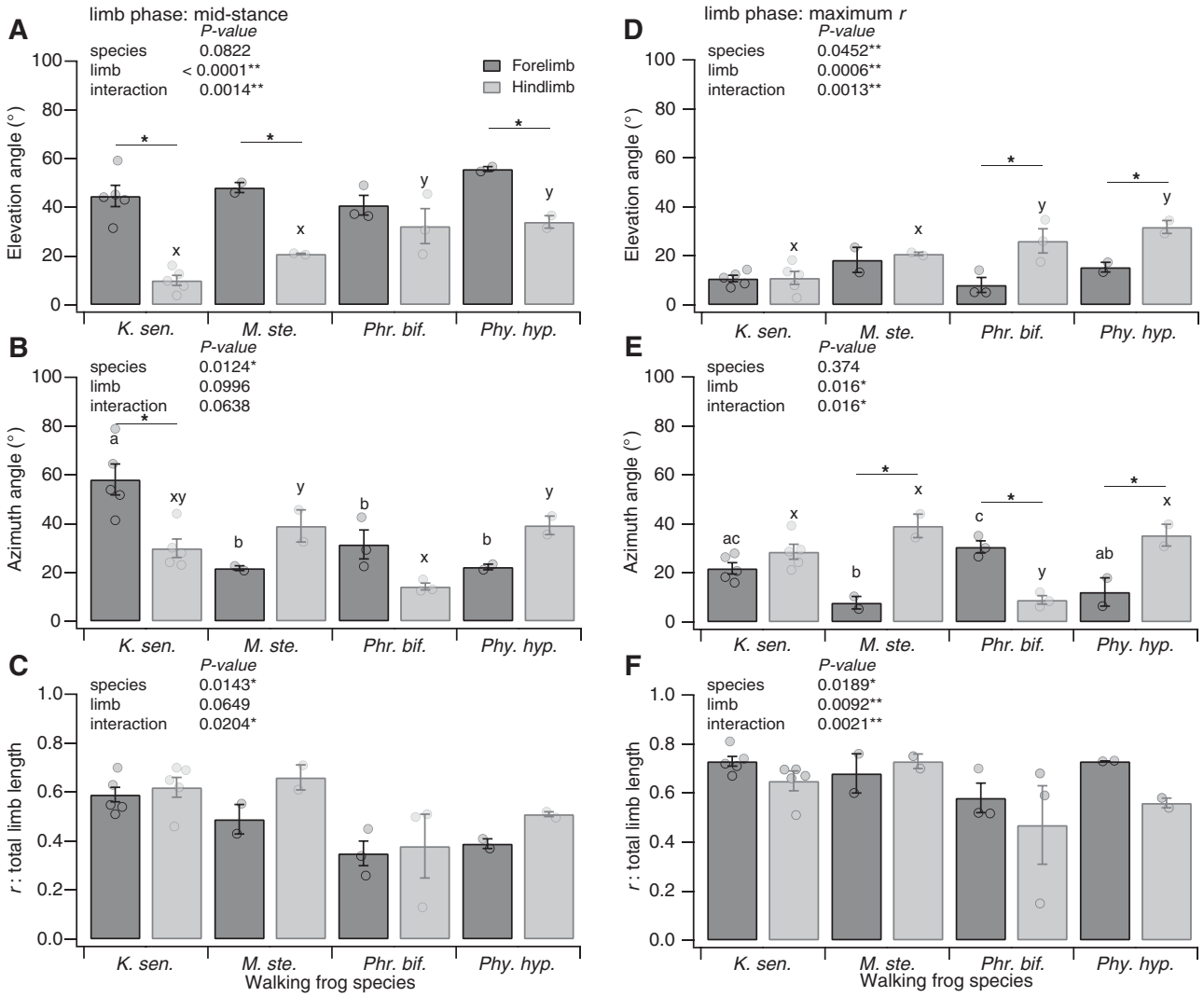

FIGURE 9 Average relative three-dimensional limb posture at mid-stance and maximum limb extension (Mean ± SEM): *Kassina senegalensis* ($n = 5$), *Melanophryniscus stelzneri* ($n = 2$), *Phrynomantis bifasciatus* ($n = 3$), and *Phyllomedusa hypochondrialis* ($n = 2$). Elevation angle, azimuth angle, and normalized radial magnitude (r) measurements of the fore- and hindlimb were taken at mid-stance of the limb (A, B, C) and at maximum limb radial extension (r) (D, E, F). P values are given for each graph. Averaged individual data points are represented as circles, see Table 1 for number of trials averaged per individual. At mid-stance, (A) elevation angle is greater in the forelimb than the hindlimb, however (B, C) there was no significant difference in azimuth angle or limb radial magnitude. During maximum r, (D) elevation angle is significantly different in the hindlimb, whereas (E) there was no significant difference in azimuth angle. Lastly, (F) relative radial magnitude is significantly different across species, however there was no difference between fore- and hindlimb. These results suggest quadrupedal walking frogs effectively use similar proportions for their fore- and hindlimb lengths across a stride, while adjusting vertical extension in the fore- and hindlimb by increasing their elevation angle throughout a stride. *Denotes significant difference within the fore- and hindlimb of a species, $P < 0.05$. Significant forelimb pairwise comparisons across species indicated with letters a, ab, b, and so on, and significant hindlimb pairwise comparisons indicated with x, y, xy, and so on. Means not sharing the same letters are significantly different (Tukey HSD, $P < 0.05$). See Supp. Table S4 for more detailed statistics

use substantial motion along other planes. There are multiple ways to achieve a "crouched" posture by using a combination of flexion, lateral abduction, or vertical retraction in a limb. We examined changes in 3D limb posture to further address our third hypothesis. We found at mid-stance the forelimb was more vertically protracted than the hindlimb (Figure 9A), with no clear difference in relative lateral abduction or adduction between the fore- and hindlimb (Figure 9B). Across the walking frog species, the effective use of the entire limb were similar in the fore- and hindlimb within a stride (Figure 9C and F). Walking frogs utilize the entire length of each limb to a similar degree. However, with slight fore–hind asymmetry in limb lengths these quadrupedal walkers seem to accommodate this length disparity in the forelimb with greater protraction in the forelimb as shown during mid-stance.

Across a stride cycle these walking frogs seem to adjust the protraction and retraction of the forelimb relative to a constantly retracted hindlimb from mid-stance to maximum extension (Figure 9A and D). This is clearly demonstrated with little changes to elevation angle in the hindlimb at mid-stance and maximum r, whereas the forelimb elevation almost doubles from maximum r to mid-stance. Similar to larger

mammals these walking anurans seem to exhibit more upright forelimb postures (Fischer, 2002; Jenkins, 1971). Adjusting for an upright forelimb posture in walking anurans likely minimizes pitch perturbations, lowers joint moments, moderates vertical forces, increases mechanical advantage, and reduces muscular loads in the forelimb (Biewener, 1983, 1989b).

We find little support that walking frog species adjust lateral abduction in the hindlimb relative to the forelimb as a mechanism to accommodate longer hindlimbs. There is little variation in azimuth angle between fore- and hindlimbs at mid-stance, however at maximum *r* the differential in azimuth angle between the fore- and hindlimb grows significant (Figure 9B and E). Quadrupedal walking frogs still utilize a sprawling gait, however may maintain a more abducted posture in the hindlimb throughout a stride in concert with a more vertically protracted forelimb, which in part allows them to accommodate for limb length asymmetries. The hindlimb vertical retraction, adjustments in forelimb protraction, and overall sprawled postures allow walking anurans to locomote with minimal pitch adjustments. Additionally, the lateral forces produced by limbs during a sprawled gait have been shown to increase stability in the horizontal plane (Kubow & Full, 1999; Schmitt & Holmes, 2000) and reduce pitching and rolling moments about the center of mass (Chen, Peattie, Autumn, & Full, 2006). Variation in limb postures may also have some important consequences for the joint moments and muscle forces required during locomotion. These changes in limb postures in the sagittal plane for walking anurans likely alter the limb effective mechanical advantage, with disproportionately retracted and flexed limbs increasing the forces and moments required to support bodyweight during locomotion (Biewener, 1989b). Similarly, a sprawled posture may reduce effective mechanical advantage and require high muscle forces. In running geckos, the abducted limb posture results in ground reaction force vectors that are oriented above the knee and elbow, and well above the hip and shoulder, thereby resulting in higher joint moments (Chen et al., 2006). Future studies focused on the effective mechanical advantage of sprawled gaits will likely elucidate the functional trade-offs associated with this common limb posture.

We initially hypothesized asymmetry in the fore- and hindlimb lengths may result in a constant downward pitch during walking. Our results do not support this hypothesis as the body pitch did not vary significantly from a horizontal orientation (Figure 7). However, we did observe somewhat substantial changes in yaw angle over a single stride (Supp. Figure S1). This observation is somewhat surprising given the short inflexible trunk of anurans. Significant changes in yaw angle are commonly observed in short limbed tetrapods with elongate bodies, where axial bending is thought to increase stride length (Ashley-Ross, 1994; Chen et al., 2006; Farley & Ko, 1997; Hildebrand, 1980). In contrast, the yaw observed in walking frogs is not likely to increase stride length significantly as it does not arise from axial bending but rather the lateral displacement of the body in response to forces generated by the hindlimbs. Since the hindlimbs are laterally displaced during walking they likely generate a relatively large mediolateral reaction force that shifts the trunk position from side to side during subsequent strides. This pattern is most notable in *Phy. hypochondrialis* where the lateral forces generated by the hindlimb shift the body over the contralateral forelimb during the period when the diagonal pair is in contact with the substrate. Although it is unclear whether the lateral displacement of the body affects stride length, it may minimize physical interference between ipsilateral limbs by tucking the forelimbs under the body and out of the way of the hindlimb.

Our results suggest specialized walkers deviate from the extreme asymmetry in fore- and hindlimb lengths common to most anurans (Figure 4; Astley, 2016). Despite this deviation, walking species still have relatively long hindlimbs and retain the ability to jump. Though performance may be somewhat compromised, changes to limb asymmetry may not directly impact jump performance but predominately affect quadrupedal walking ability. For example, we have observed *K. senegalensis*, *M. stelzneri*, and *Phy. hypochondrialis* not limited to walking locomotion but also run, swim, and jump (personal observation). As seen in another specialized anuran walker, *K. maculata* maintains average jumping capabilities in comparison with other anurans (Porro, Collings, Eberhard, Chadwick, & Richards, 2017). In contrast, Astley (2016) found walkers tend to have inferior jump performance and shorter hindlimb lengths relative to body length. Since asymmetry in limb length appears to be maintained to preserve jumping performance as a predator avoidance strategy, then quadrupedal walkers need to make kinematic adjustments to accommodate their body plan. We show that one strategy used by four walking species is to reduce the vertical protraction of their relatively long hindlimbs and locomote with a highly-protracted forelimb posture similar to cursorial mammals (Schmidt, 2005).

Specialized walkers show modifications to limb length and kinematics on local and evolutionary timescales. Although a sprawled posture has benefits, it also creates larger bending loads and subsequently alters mechanical advantage and ground reaction forces. This shift of specialized characteristics for jumping to walking in anurans provides another example of the difficulties in "re-evolving quadrupedal walking." In a similar case, vampire bats specialized for flight, have independently evolved a bounding gait (Riskin & Hermanson, 2005). Bats have highly elongated forelimbs, a mechanical adaptation for flight, but no more elongated than brachiating or knuckle-walking primates (Swartz, 1997; Swartz & Middleton, 2007). Such limb asymmetries may have implications for a quadrupeds' choice in gait and limb posture. These transitions between locomotor modes and limb adaptations offers insight into the timescale of modifications across tetrapod gaits and the associated trade-offs. Our study offers a basis for understanding the conflicts across diverse locomotor modes, and how novel gaits shape limb morphology, kinematics, and motor control strategies.

ACKNOWLEDGMENTS

We are grateful to Greg Pauly, the assistant curator, and Neftali Camacho, collections manager, of Herpetology, Los Angeles County Museum of Natural History (LACM) for access to specimens. We thank doctoral committee members for CMR (Matt McHenry and Donovan German), Thomas Roberts for advice and mentorship to HCA, as well as Caitrin Eaton, Nicole Danos, and Joseph Heras for useful discussions and insights. Additionally, we are thankful to Marla

Goodfellow, Yasmin Gutierrez, Ashley Hughes, and Priyanka Satish for help with animal husbandry and data collection.

AUTHOR CONTRIBUTIONS

C.M.R. and E.A. conceived the study; C.M.R. and H.C.A. carried out experiments; C.M.R. analyzed data; C.M.R. and E.A. drafted the manuscript; C.M.R., H.C.A., and E.A. edited the manuscript.

ORCID

Crystal M. Reynaga http://orcid.org/0000-0003-3264-5658

REFERENCES

Aerts, P. (1998). Vertical jumping in *Galago senegalensis*: The quest for an obligate mechanical power amplifier. *Philosophical Transactions of the Royal Society B: Biological Sciences*, *353*(1375), 1607–1620. https://doi.org/10.1098/rstb.1998.0313

Ahn, A. N., Furrow, E., & Biewener, A. A. (2004). Walking and running in the red-legged running frog, *Kassina maculata*. *Journal of Experimental Biology*, *207*, 399–410. https://doi.org/10.1242/jeb.00761

Ashley-Ross, M. A. (1994). Hindlimb kinematics during terrestrial locomotion in a salamander (*Dicamptodon tenebrosus*). *Journal of Experimental Biology*, *193*(1), 255–283.

Astley, H. C. (2016). The diversity and evolution of locomotor muscle properties in anurans. *Journal of Experimental Biology*, *219*, 3163–3173. https://doi.org/10.1242/jeb.142315

Biewener, A. A. (1983). Allometry of quadrupedal locomotion: The scaling of duty factor, bone curvature and limb orientation to body size. *Journal of Experimental Biology*, *105*, 147–171.

Biewener, A. A. (1989a). Mammalian terrestrial locomotion and size. *Bioscience*, *39*(11), 776–783. https://doi.org/10.2307/1311183

Biewener, A. A. (1989b). Scaling body support in mammals: Limb posture and muscle mechanics. *Science*, *245*(4915), 45–48. https://doi.org/10.1126/science.2740914

Biewener, A. A. (2005). Biomechanical consequences of scaling. *Journal of Experimental Biology*, *208*(9), 1665–1676. https://doi.org/10.1242/jeb.01520

Chen, J. J., Peattie, A. M., Autumn, K., & Full, R. J. (2006). Differential leg function in a sprawled-posture quadrupedal trotter. *Journal of Experimental Biology*, *209*, 249–259. https://doi.org/10.1242/jeb.01979

Chen, J., Bever, G. S., Yi, H. Y., & Norell, M. A. (2016). A burrowing frog from the late Paleocene of Mongolia uncovers deep history of spadefoot toads (Pelobatoidea) in East Asia. *Scientific Reports*, *6*, 19209. https://doi.org/10.1038/spe19209.

Choi, I., Shim, J. H., & Ricklefs, R. E. (2003). Morphologic relationships of take-off speed in anuran amphibians. *Journal of Experimental Zoology A*, *299*(2), 99–102. https://doi.org/10.1002/jez.a.10293

Emerson, S. B. (1976). Burrowing in frogs. *Journal of Morphology*, *149*(4), 437–458. https://doi.org/10.1002/jmor.1051490402

Emerson, S. B. (1979). The ilio-sacral articulation in frogs: Form and function. *Biological Journal of the Linnean Society*, *11*, 153–168. https://doi.org/10.1111/j.1095-8312.1979.tb00032.x

Emerson, S. B. (1988). Convergence and morphological constraint in frogs: Variation in postcranial morphology. *Fieldiana Zoology*, *43*, 1–19.

Emerson, S. B., & Koehl, M. A. R. (1990). The interaction of behavioral and morphological change in the evolution of a novel locomotor type: "Flying" frogs. *Evolution*, *44*(8), 1931–1946. https://doi.org/10.1111/j.1558-5646.1990.tb04300.x

Farley, C. T., & Ko, T. C. (1997). Mechanics of locomotion in lizards. *Journal of Experimental Biology*, *200*(16), 2177–2188.

Fischer, M. S., Schilling, N., Schmidt, M., Haarhaus, D., & Witte, H. (2002). Basic limb kinematics of small therian mammals. *Journal of Experimental Biology*, *205*(9), 1315–1338.

Frost, D. R., Grant, T., Faivovich, J., Bain, R. H., Haas, A., Haddad, C. F. B., … Ward, C. (2006). The amphibian tree of life. *Bulletin of the American Museum of Natural History*, *297*, 8–370.

Gans, C., & Parsons, T. S. (1966). On the origin of the jumping mechanism in frogs. *Evolution*, *20*, 92–99. https://doi.org/10.1111/j.1558-5646.1966.tb03345.x

Garland, T., Jr., & Ives, A. R. (2000). Using the past to predict the present: Confidence intervals for regression equations in phylogenetic comparative methods. *The American Naturalist*, *155*(3), 346–364.

Gomes, F. R., Rezende, E. L., Grizante, M. B., & Navas, C. A. (2009). The evolution of jumping performance in anurans: Morphological correlates and ecological implications. *Journal of Evolutionary Biology*, *22*(5), 1088–1097. https://doi.org/10.1111/j.1420-9101.2009.01718.x

Grafen, A. (1989). The phylogenetic regression. *Philosophical Transactions of the Royal Society B: Biological Sciences*, *326*(1233), 119–157. https://doi.org/10.1098/rstb.1989.0106

Hedrick, T. L. (2008). Software techniques for two- and three-dimensional kinematic measurements of biological and biomimetic systems. *Bioinspiration & Biomimetics*, *3*(3), 034001. https://doi.org/10.1088/1748-3182/3/3/034001

Hildebrand, M. (1968). Symmetrical gaits of dogs in relation to body build. *Journal of Morphology*, *124*(3), 353–360. https://doi.org/10.1002/jmor.1051240308

Hildebrand, M. (1980). The adaptive significance of tetrapod gait selection. *American Zoologist*, *20*(1), 255–267.

Hildebrand, M. (1985). Walking and running. In M. Hildebrand, D. M. Bramble, K. F. Liem, & D. B. Wake (Eds.), *Functional vertebrate morphology* (pp. 38–57). Cambridge, MA: Harvard University Press.

Isaac, N. J. B., Redding, D. W., Meredith, H. M., & Safi, K. (2012). Phylogenetically-Informed Priorities for Amphibian Conservation. *PLoS ONE*, *7*(8), e43912. https://doi.org/10.1371/journal.pone.0043912

Jenkins, F. A. (1971). Limb posture and locomotion in the Virginia opossum (*Didelphis marsupialis*) and in other non-cursorial mammals. *Journal of Zoology*, *165*(3), 303–315. https://doi.org/10.1111/j.1469-7998.1971.tb02189.x

Jenkins, F. A., & Shubin, N. H. (1998). *Prosalirus bitis* and the anuran caudopelvic mechanism. *Journal of Vertebrate Paleontology*, *18*(3), 495–510. https://doi.org/10.1080/02724634.1998.10011077

Jorgensen, M. E., & Reilly, S. M. (2013). Phylogenetic patterns of skeletal morphometrics and pelvic traits in relation to locomotor mode in frogs. *Journal of Evolutionary Biology*, *26*(5), 929–943. https://doi.org/10.1111/jeb.12128

Kubow, T. M., & Full, R. J. (1999). The role of the mechanical system in control: A hypothesis of self-stabilization in hexapedal runners. *Philosophical Transactions of the Royal Society B: Biological Sciences*, *354*(1385), 849–861. https://doi.org/10.1098/rstb.1999.0437

Marsh, R. L. (1994). Jumping ability of anuran amphibians. *Advances in Veterinary Science Comparative Medicine*, *38B*, 51–111.

Martins, E. P., & Hansen, T. F. (1997). Phylogenies and the comparative method: A general approach to incorporating phylogenetic information into the analysis of interspecific data. *The American Naturalist*, *149*(4), 646–667. https://doi.org/10.1086/286013

Napier, J. R., & Walker, A. C. (1967). Vertical clinging and leaping—A newly recognized category of locomotor behavior of primates. *Folia Primatologica*, *6*(3), 204–219. https://doi.org/10.1159/000155079

Orme, D., Frechketon, R. P., Thomas, G. H., Petzoldt, T., Fritz, S., Isaac, N., & Pearse, W. (2013). Caper: Comparative analysis of phylogenetics and evolution in R. version 0.5.2.

Paradis, E., Claude, J., & Strimmer, K. (2004). APE: Analysis of phylogenetics and evolution in R language. *Bioinformatics*, *20*(2), 289–290. https://doi.org/10.1093/bioinformatics/btg412

Peplowski, M. M., & Marsh, R. L. (1997). Work and power output in the hindlimb muscles of Cuban tree frogs *Osteopilus septentrionalis* during jumping. *Journal of Experimental Biology*, *200*(22), 2861–2870.

Pinheiro, J., Bates, D., DebRoy, S., & Sarkar, D. & R Development Core Team. (2017). nlme: Linear and nonlinear mixed effects models. *R package version*, *3*, 1–131.

Porro, L. B., Collings, A. J., Eberhard, E. A., Chadwick, K.P., & Richards, C. T. (2017). Inverse dynamic modelling of jumping in the red-legged running frog, *Kassina maculata*. *Journal of Experimental Biology*, *220*, 1882–1893. https://doi.org/10.1242/jeb.155416

Preuschoft, H., Witte, H., & Fischer, M. (1995). Locomotion in nocturnal prosimians. In L. Alterman, G. A. Doyle, & M. Kay (Eds.), *Creatures of the dark: The nocturnal prosimians* (pp. 453–472). Boston, MA: Springer US. https://doi.org/10.1007/978-1-4757-2405-9_27

Reilly, S. M., & Jorgensen, M. E. (2011). The evolution of jumping in frogs: Morphological evidence for the basal anuran locomotor condition and the radiation of locomotor systems in crown group anurans. *Journal of Morphology*, *272*(2), 149–168. https://doi.org/10.1002/jmor.10902

Reilly, S. M., McElroy, E. J., Odum, R. A., & Hornyak, V. A. (2006). Tuataras and salamanders show that walking and running mechanics are ancient features of tetrapod locomotion. *Proceedings of the Royal Society B: Biological Science*, *273*(1593), 1563–1568. https://doi.org/10.1098/rspb.2006.3489

Riskin, D. K., & Hermanson, J. W. (2005). Independent evolution of running in vampire bats. *Nature*, *434*(7031), 292. https://doi.org/10.1038/434292a

Rohlf, F. J. (2001). Comparative methods for the analysis of continuous variables: Geometric interpretations. *Evolution*, *55*(11), 2143–2160.

Schmidt, M. (2005). Hind limb proportions and kinematics: Are small primates different from other small mammals? *Journal of Experimental Biology*, *208*(17), 3367–3383. https://doi.org/10.1242/jeb.01781

Schmitt, J., & Holmes, P. (2000). Mechanical models for insect locomotion: Dynamics and stability in the horizontal plane—II. Application. *Biological Cybernetics*, *83*(6), 517–527. https://doi.org/10.1007/s004220000180

Shubin, N. H., & Jenkins, F. A. (1995). An early Jurassic jumping frog. *Nature*, *377*, 49–52. https://doi.org/10.1038/377049a0

Steudel, K., & Beattie, J. (1993). Scaling of cursoriality in mammals. *Journal of Morphology*, *217*(1), 55–63. https://doi.org/10.1002/jmor.1052170105

Swartz, S. M. (1997). Allometric patterning in the limb skeleton of bats: Implications for the mechanics and energetics of powered flight. *Journal of Morphology*, *234*(3), 277–294. https://doi.org/10.1002/(SICI)1097-4687(199712)234:3<277::AID-JMOR6>3.0.CO;2-6

Swartz, S. M., & Middleton, K. M. (2007). Biomechanics of the bat limb skeleton: Scaling, material properties and mechanics. *Cells Tissues Organs*, *187*(1), 59–84. https://doi.org/10.1159/000109964

Zug, G. R. (1972). Anuran locomotion: Structure and function. I. Preliminary observations on relation between jumping and osteometrics of appendicular and postaxial skeleton. *Copeia*, *4*, 613–624. https://doi.org/10.2307/1442720

Zug, G. R. (1978). Anuran locomotion— structure and function. 2: Jumping performance of semiaquatic, terrestrial, and arboreal frogs. *Smithsonian Contributions to Zoology*, *276*, 1–31.

SUPPORTING INFORMATION

Additional supporting information may be found online in the Supporting Information section at the end of the article.

How to cite this article: Reynaga CM, Astley HC, Azizi E. Morphological and kinematic specializations of walking frogs. *J Exp Zool*. 2018;329:87–98. https://doi.org/10.1002/jez.2182